Article

Forest Dynamics and Agroforestry History since AD 200 in the Highland of Sumatra, Indonesia

Chung Hoai Nguyen [1,*], Christina Ani Setyaningsih [1,2], Svea Lina Jahnk [1], Asmadi Saad [3], Supiandi Sabiham [4] and Hermann Behling [1]

1 Department of Palynology and Climate Dynamics, Albrecht-von-Haller-Institute for Plant Sciences, University of Göttingen, Untere Karspüle 2, 37073 Göttingen, Germany
2 Research and Development Center for Oil and Gas Technology, The Ministry of Energy and Mineral Resources of Indonesia. Jl. Ciledug Raya kav. 109, Cipulir, Kebayoran Lama, Jakarta Selatan 12230, Indonesia
3 Department of Soil Science, University of Jambi (UNJA), Jalan Raya Jambi Muara Bulian KM 15 Mandalo Darat, Jambi 36361, Indonesia
4 Department of Soil Science and Land Resource, Bogor Agriculture University (IPB), Jalan Meranti, IPB Campus, Darmaga, Bogor 16680, Indonesia
* Correspondence: chung-hoai.nguyen@biologie.uni-goettingen.de

Abstract: Understanding past forest dynamics and human influence is essential for future forest management and ecosystem conservation. This study aims to provide insights into the forest dynamics and agroforestry history in the highlands of Sumatra for the last 1800 years. We carried out palaeoecological multi-proxy analyses of pollen, spores, non-pollen palynomorphs, macro-charcoal, and X-ray fluorescence on a limnic sediment core taken from Danau Kecil in the submontane area of Kerinci Seblat National Park in Sumatra, Indonesia. Our results provide an 1800-year record of forest dynamics under climate change and human influence including the transition from forest opening to shifting cultivation and eventually permanent agroforestry. Indicators for forest openings and secondary forest formation have been present since the beginning of records (AD 200). This is followed by the possible initiation of sugar palm (*Arenga*) cultivation (AD 400). Since AD 500, potential agroforestry and forest gardening practices have promoted major timber trees such as *Lithocarpus/Castanopsis, Bischofia*, and Dipterocarpaceae combined with sugar palm (*Arenga*). Permanent agroforestry systems were possibly established since AD 1760, evinced by an increase in commodity trees such as Dipterocarpaceae for resin production. With the Dutch invasion ca. AD 1900, agroforestry intensified and expanded to the Kerinci Valley. This was followed by land use intensification and potential rice cultivation around Danau Kecil since the 1940s. This study provides the first details on past forest dynamics around Danau Kecil since AD 200, showing among others how appropriate forest management and a closed canopy could reduce fire vulnerability in submontane rainforest.

Keywords: tropical forest; late Holocene; land use; forest transformation; forest cultivation; Sumatra; Indonesia

1. Introduction

Indonesia is one of the major producers and exporters of agricultural products worldwide. Products such as rubber, tea, palm oil, coffee, cocoa, spices, cassava, and cinnamon have become the main drivers of economic growth and livelihoods for great parts of the Indonesian population in the past decades [1]. Early farming or initial agriculture in Indonesia was thought to start in mountainous areas with the shifting cultivation of root crops and the cultivation of swamps. However, little is known about when and where those activities occurred, except for the evidence of deforestation and burning about 2000 BC [2,3]. Afterward, with the arrival of Austronesian migrants in ca. 1550 BC, rice cultivation was introduced [2,4]. Within Indonesia, Sumatra offers ideal conditions for agriculture due

to its humid tropical climate and fertile volcanic soils. Evidence shows a long history of human occupation in the Kerinci area, with archaeological finds dating back to 1400 BC [5]. However, the history of agricultural practices in Sumatra is still understudied. Aside from evidence of rice cultivation at the Toba Plateau in North Sumatra [2] and Danau Bento in the Kerinci Seblat National Park (KSNP) [4], there is no further indication of the past cultivation of other crops in Sumatra.

In recent years, agricultural activities in Indonesia have been rapidly expanding. Especially in Sumatra, the rainforest has been extensively transformed toward cash crop-oriented monocultures such as oil palm and cinnamon plantations. Meanwhile, the ecological impact of land-use transformation and deforestation have attracted global attention, whereby the consequences of climate change and anthropogenic disturbances are threatening not only ecosystems, but also human welfare [6,7]. One of these threats is reflected in the recently increasing wildfire risk in Indonesia. Since Southeast Asian rainforests thrive under constantly humid conditions, fires did not play a significant role in the past [8]. However, since the major expansion of agricultural areas on islands such as Sumatra, the land-use fragmentation and drainage of peatland led to a severe increase in fire frequency and magnitude [9,10]. In 1997/1998, Indonesia counted the highest number of fires worldwide, causing forest fire control to be one of the highest priorities at the Ministry of Forest in Indonesia [9]. There have been various studies addressing the fire problem [11–14]. However, limited knowledge on fire dynamics including the causes and ecological magnitude of fires cause management efforts to be less effective. Therefore, an understanding of the role of fires in tropical forest ecosystem dynamics must precede efforts in fire management and control. This comprises the separation of natural (e.g., drought, high rainfall) and anthropogenic (e.g., landscape fragmentation) fire risks as well as the relationship between fire and tropical rainforests.

The objective of this study was to provide information of submontane forest dynamics under the effect of fire, climate, and human activities to support future fire control and forest management strategies in the face of rapid landscape change and increasing fire risks. We conducted a paleoecological study on a core taken from submontane Danau Kecil of KNSP in Jambi to understand: (i) the submontane vegetation, fire, and climate dynamics in KSNP over the last 2000 years; (ii) the effect of human activities and agricultural practices on the submontane rainforest around Danau Kecil over the last 2000 years; and (iii) the past land use dynamics regarding the forest management strategies and forest recovery phases of submontane forest around Danau Kecil. In the paleoecological approach, we used pollen and spores to reconstruct the vegetation changes and climatic conditions. Macro-charcoal analysis was used to reconstruct the local fire regime. Fossil remains of the mycorrhiza-fungi "*Glomus*" are used as an indicator of erosion, and X-ray fluorescence (XRF) analysis is used to interpret disturbances in the lake catchment (e.g., past environmental and climate change; anthropogenic activities). The outcome of this study provides supportive information for future forest management to rehabilitate, restore, and conserve the submontane ecosystem including fire control and sustainable development strategies in the future.
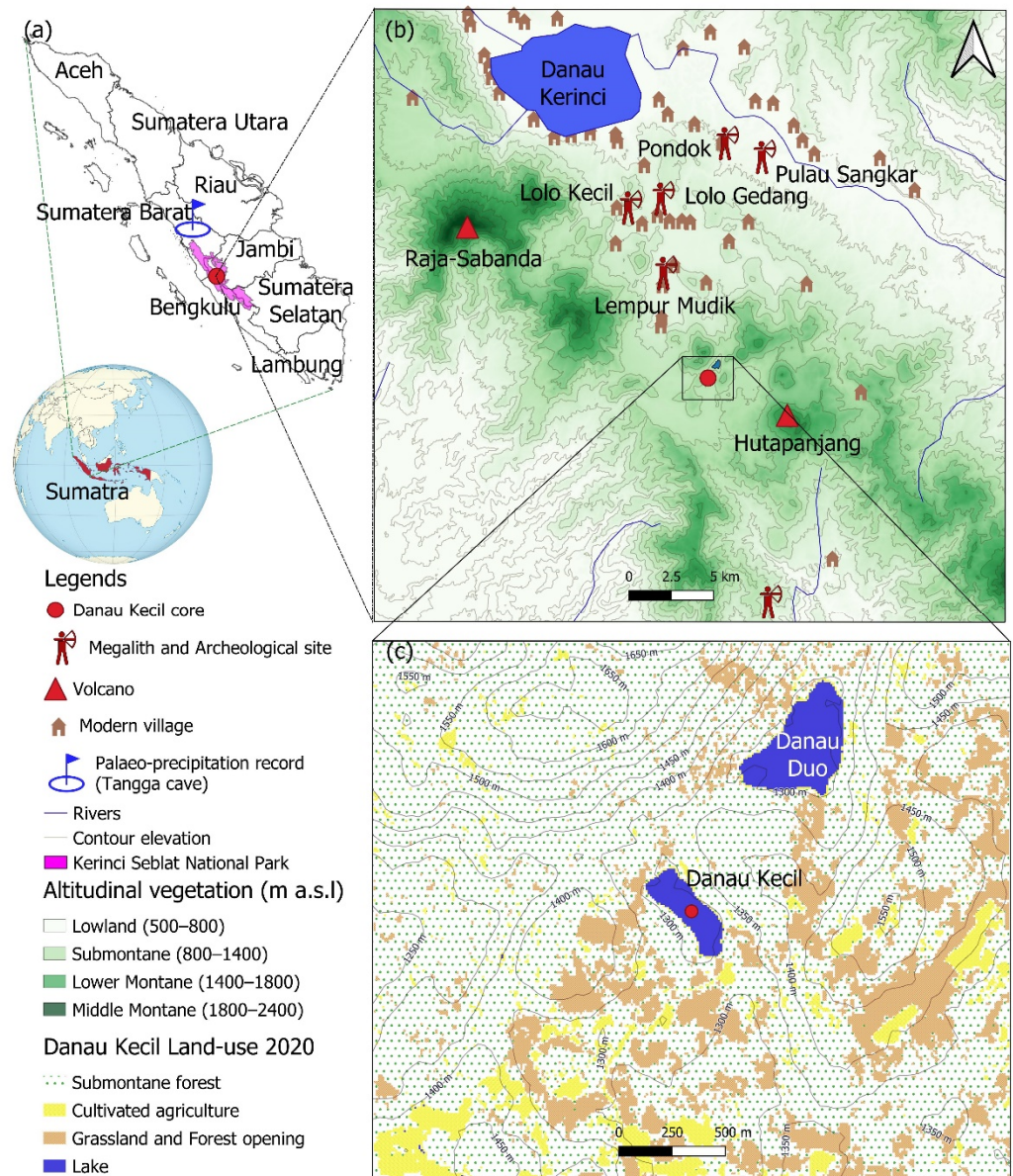
2. Study Area

2.1. Geography Setting

Sumatra Island forms a biogeographic region between the Asian mainland in the west and the area of Sundaland in the east [15]. The western part of this island is dominated by the Barisan mountain range, running along the whole length of Sumatra [16]. A major part of the Barisan Mountains is covered by the Kerinci Seblat National Park (KSNP), a biodiversity hotspot, and the largest national park in Sumatra [17].

The lake Danau Kecil (DK) in the KSNP lies at an elevation of 1285 m a.s.l. (Figure 1). The lake is located about 20 km south of the largest highland lake in Sumatra, Danau Kerinci. DK is ca. 70 m long and ca. 390 m wide, with a maximum water depth of 12.5 m. The site is surrounded by rolling hills, partly covered by cinnamon (*Cinnamommum burmanii*) agroforestry and submontane tropical forest. The regional submontane vegetation is

dominated by Fagaceae, Myrtaceae, Lauraceae, Moraceae, and Rubiaceae. Secondary forest formations as part of the submontane forest majorly consist of Euphorbiaceae (*Macaranga*), Urticaceae, Moraceae (*Ficus*), Ulmaceae (*Trema*), and Gleicheniaceae [15,18]. Nowadays, the submontane forests surrounding DK have been greatly converted into settlements, cultivated land, and agroforestry (Figure 1c).

Figure 1. Map of the study area. (**a**) Location of the studied region, pink area of the Kerinci Seblat National Park (KSNP) in Sumatra. The red dot shows the location of the study site (Danau Kecil) in the KSNP and the paleo-precipitation record in the Tangga Cave [19]. (**b**) The study site: The Danau Kecil core is marked by the red dot. The red triangles represent unactive volcanoes. Information on the location of archeological sites and modern villages was derived from Bonatz [5] and Aziz [20]. Data source for the digital elevation model: ASTER GDEM Version 2 from METI and NASA, altitudinal vegetation types were adapted from Laumonier [15], and the location of volcanoes were from the Global Volcanism Program [21]-https://volcano.si.edu/ (accessed on 24 August 2021). (**c**) Land-use map around Danau Kecil was derived from Sentinel satellite images (USGS database, https://earthexplorer.usgs.gov; 2020). Dot areas indicate submontane forest, orange areas indicate grassland and open forest; yellow areas indicate agricultural cultivated land.

2.2. Climate

The Sumatran climate can be classified as a full humid equatorial rainforest climate (Köppen: Af; [22,23]). Due to its location between the Indian and Pacific Oceans, Sumatra is influenced by the El Niño Southern Oscillation (ENSO) and the Indian Ocean Dipole (IOD). During the El Niño warm phase, Sumatra receives less rainfall than in other years. Reversely, during the La Niña cold phase, there is higher rainfall in the region [24,25]. The IOD is a non-periodic oscillation of sea-surface temperatures in the Indian Ocean. Cooling waters in the eastern Indian Ocean and droughts in Sumatra are associated with a positive phase of IOD. The negative phase of IOD brings the opposite phenomenon [26]. According to rainfall data observed from 1970 to 2000 ([27]; WorldClim–Global Climate Data, http://www.worldclim.org/), the study area has an average temperature of 19 °C, which changes little during the year and a high annual precipitation rate of 2351 mm yr^{-1}. The dry season occurs from June to August with less precipitation (ca. 100–150 mm yr^{-1}), and the major rainy season takes place from October to May.

2.3. History of Agriculture and Land-Use System

Previous palynological investigations in KSNP have shown that forest clearance was evident at least since 2050 BC [18,28]. This period concurred with the migration of Austronesian-speaking people to Borneo, Java, Sumatra, and the Peninsular Malaysia from Taiwan, known as "the early farming dispersal", about 1550 BC [3,29]. The Austronesians can be considered as the first inhabitants to engage in agricultural activities and early farming in Sumatra. Consequently, food production from cultivation gradually replaces the pre-existing hunter–gatherer activities [29]. These early farming communities marked the emergence of the local Neolithic period, a crucial event in the history of human occupation in Indonesia [30], indicated by the archeological remains such as axes, pottery, mats, and nets [16]. Most of the cultivation systems in the area of Austronesian residence were characterized by shifting and localized swamp cultivation [3]. This cultivation type is substantiated by evidence of rice cultivation in Sumatra, provided by the paleoecological studies of Danau Bento and the Toba Plateau [2,4]. However, evidence of cultivation associated with permanent forest clearing, which can better attest to the beginning of permanent agroforestry, started only about 3000 years ago [3,18,31]. The Bronze–Iron Age [31] is marked by archeological evidence of elaborate pots and early metalwork [32]. During this cultural phase, humans cultivated rice and other crop plants and were known as cultivators [16,29].

The Sumatran Bronze and Iron age is followed by the "Megalithic period" from the 10th until the 14th century AD, peaking during the 12th century AD. This period is marked by archeological finds of stone megaliths and specific burial jars, whereas excavations at Renah Kemumu, Serampas, and Lolo Gedang revealed the remnants of stone housing during that time [5,33]. Subsequently, during the era of colonialism, the agricultural system in Indonesia experienced extensive transformation. Traditional crops such as eggplant (*Solanum melongena* L.), long beans (*Vigna* spp. L.), and papaya (*Carica papaya* L.) were exchanged for valuable cash crops of global interest. These included coffee (*Coffea canephora* Pierre ex A. Froehner, *C. arabica* L.), cinnamon (*Cinnamomum burmanii* Nees & T. Nees), rubber (*Hevea brasiliensis Willd*), tea (*Camellia sinensis* L.), oil palm (*Elaeis guineensis* Jacq.), sugar palm (*Arenga pinnata* Wurmb.), and damar resin (*Shorea javanica* Koord & Valenton) [15,34,35].

3. Materials and Methods

3.1. Fieldwork, Sediment Description and Dating

The 298 cm long sediment core of Danau Kecil (DK; 101°33′28.45″ S, 2°18′36.59″ E) was recovered from the center of the lake (deepest part) in August 2017 by using a Livingstone piston corer [36]. The coring was conducted as part of a field work campaign by CRC990-EFForTS subproject A01. Established in 2012, the Collaborative Research Center 990 focuses on ecological and socioeconomic functions and trade-offs of tropical lowland rainforest and

transformation systems (short EFForTS), with subproject A01 addressing the long-term vegetation dynamics, plant phenology, and plant–pollinator interactions in rainforest and rainforest transformations in central Sumatra. Cores were stored under cold (+4 °C) and wet conditions.

The sediments mainly consist of organic silt with the presence of charcoal and plant fragments (Figure 2). The lowermost layer (298–220 cm) consists of brownish-black silt, with a high proportion of plant fragments and some fine charcoal debris. The middle core part (220–100 cm) consisted of dusky-brown silt with small and occasionally bigger plant fragments. The uppermost part (100–0 cm) presented a fluctuation of dusky-yellowish-brown, greyish-brown, brownish-black, brownish-grey, and dusky-brown silt with a high proportion of charcoal and leaf fragments. Sedimentological descriptions and symbols are illustrated in Sedlog version 3.1 [34]. Eight samples of plant remains, and organic bulk sediment were sent to the Poznan Radiocarbon Laboratory in Poland for radiocarbon dating (Table 1). The age was calibrated using the Southern Hemisphere SHCal13.14C calibration curve [35]. The age–depth model was performed using the Clam version 2.3.2 [37] script in R [38].
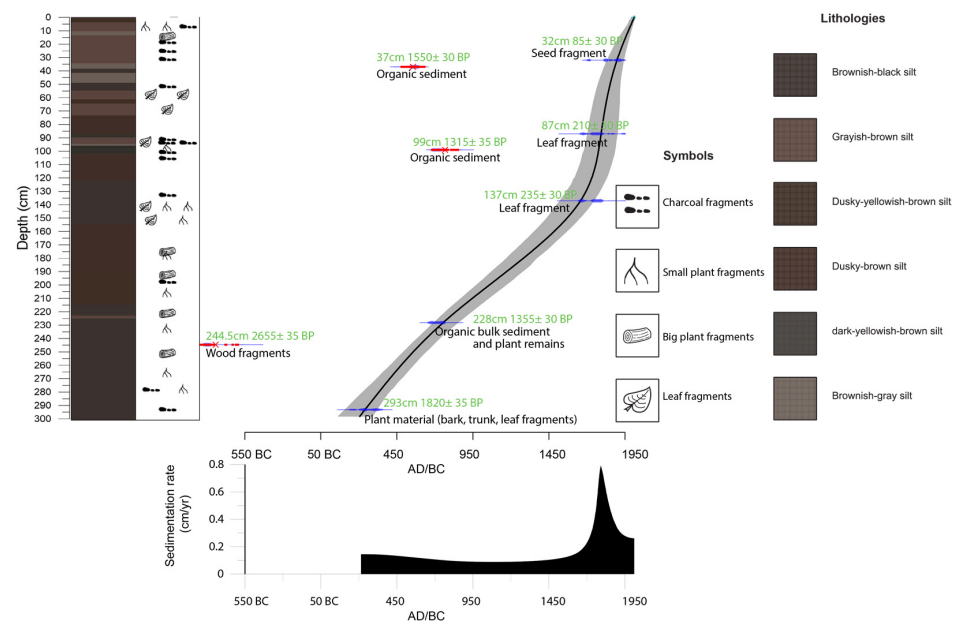
Figure 2. The lithology and age–depth model of the DK core. Red points represent the outliers.

Table 1. A list of the radiocarbon dates from the DK core.

No.	Lab Code	Depth	Material	^{14}C yr BP	cal. yr BP	Calendar Age (AD)
1	Poz-140430	32 cm	Plant remains (seed fragment)	85 ± 30	53	1897
2	Poz-132660	37 cm	Organic bulk sediment	1550 ± 30		
3	Poz-141013	87 cm	Plant remains (leaf fragment)	210 ± 30	157	1793
4	Poz-132661	99 cm	Organic bulk sediment	1315 ± 30		
5	Poz-140493	137 cm	Plant remains (leaf fragment)	235 ± 30	292	1658
6	Poz-132645	228 cm	Organic bulk sediment and plant remains	1355 ± 30	1196	754
7	Poz-140517	244.5 cm	Plant remains (wood fragment)	2655 ± 35		
8	Poz-101166	293 cm	Plant material (bark, trunk, leaf fragments)	1820 ± 35	1710	240

3.2. Palynological Analysis

A total of 40 samples of the 298 cm long sediment core were taken for palynological analysis in 8 cm intervals. Each sample, consisting of 0.5 cm^3 of sediment, was processed

using standard palynological methods following Faegri & Iversen [39]. Pollen and spore counting was carried out using a light microscope. The pollen grains were counted to a minimum of 300 grains per sample excluding aquatic pollen, spores, and non-pollen palynomorphs (NPPs). Pollen and spore identification was based on the modern tropical pollen reference collection from Sumatra of the Department of Palynology and Climate Dynamics of the University of Göttingen (https://www.uni-goettingen.de/de/97306.html) and the Australasian Pollen and Spore Atlas (APSA; https://apsa.anu.edu.au/samples/. All pollen and spore taxa were included in the analysis in which pollen percentages were calculated relative to the total pollen sum, and fern spores were calculated as the percentage of the total pollen and spore sum. Pollen and spore concentrations were calculated using the exotic marker *Lycopodium clavatum* [40] and expressed as the number of pollen grains and spore grains per cm^3. The software StrataBugs$^®$ v.2.1 [41] was used to create the pollen diagram. A few taxa with similar morphology and therefore difficult to separate were grouped together such as Moraceae/Urticaceae excluding *Ficus*, *Lithocarpus/Castanopsis*, and *Mallotus/Macaranga*. Local pollen zones were defined by a cluster analysis, performed on percentages of all terrestrial pollen using CONISS [42].

3.3. Macro-Charcoal Analysis

Macro-charcoal particles (>125 μm) were analyzed in continuous 1 cm intervals along the core (total 296 samples). Samples of 1 cm^3 were processed following the method of Stevenson and Haberle [43]. Samples were soaked in a 5% sodium hexametaphosphate solution ($NaPO_3$) to help disaggregate the samples and remove charcoal particles from the other material. After removing $NaPO_3$, customary bleach was added to remove all organic material, highlighting dark, inorganic material such as charcoal. The samples were sieved through a 125 μm mesh to remove smaller particles (long distance "background signal") for a more local charcoal signal [44,45]. The remaining charcoal particles were identified and counted under a binocular stereomicroscope. The local fire regime was reconstructed using the CharAnalysis software [46] with threshold values on a percentile cut-off of noise distribution, modeled with a 0- or 1-mean Gaussian and 500 yr to smooth over the fire frequency and fire return intervals. The raw charcoal counting was interpolated to 7 year intervals (the median temporal resolution). The charcoal accumulation rate was expressed as the number of particles cm^{-2} yr^{-1}.

3.4. X-ray Fluorescence (XRF) Analysis

XRF scans were performed at the Department for Geomorphology and Polar research, University of Bremen, Germany. The XRF elements were measured in counts per second (cps). Ti, Fe, Zr, K, Pb, Ca, Zn, and Cu were the most dominant elements obtained from the XRF scanning. In addition, the ratio of Al/K, Rb/Sr, and CIA was calculated to evaluate the degree of chemical weathering [47–49]. The CIA calculation was initially proposed by Nesbitt and Young [50] and defined as the relative abundance of [Al/(Al + Na + Ca + K)] × 100.

3.5. Multivariate Statistical Analysis

Multivariate statistical analysis has been conducted to detect the most dominant environmental factors that are driving vegetation dynamics over time. Identified pollen and spores were included as relative abundance in the analysis. An unconstrained principal component analysis (PCA) and detrended correspondence analysis (DCA) were performed to detect patterns in the pollen and spore composition. Pollen and spore data were square-root transformed to reduce the effect of a skewed abundance distribution and zero values in the record [51,52]. Furthermore, a constrained ordination (redundancy analysis (RDA)) was carried out to extract the variation, which can be directly explained by the environmental variables. The following environmental variables were used: fire frequency as an indicator of local fire dynamics, *Glomus* concentration as an indicator of soil erosion, and XRF elements such as Ti, Si, Fe, Zr, and K as indicators of siliciclastic input into the lake sediment [53,54]. PCA and RDA were computed using CANOCO 5 [52]. In addition, a sim-

ple linear regression was applied to illustrate the relationship between fire frequency from CharAnalysis [46], paleo-precipitation data from Wurtzel, et al. [19], and pollen and spore data in percentage. The linear regression model was performed using Grapher^{TM} from Golden Software, LLC (https://www.goldensoftware.com accessed on 24 August 2021).

4. Results

4.1. Age-Depth Model

The chronology of the DK core was obtained from eight radiocarbon dates (Table 1). Only radiocarbon dates from macrofossils were accounted in the analysis. Two radiocarbon dates of the organic bulk sediment samples (Poz-132660, Poz-132661) taken from the upper part of the core were excluded, as the sediment layers here (Figure 2) implied possible fluctuation. The radiocarbon date of the sample Poz-140517 was flagged as an outlier due to the too-old age. The depth versus age relationship was fitted into a smooth spline model (Figure 2), suggesting an irregular sediment accumulation in the last 1800 years (AD 200 to present). From AD 200–1700 (298–122 cm), the sediment accumulation rate was low, with ca. 0.14 cm yr^{-1}. The sediment accumulation rate then strongly increased to ca. 0.54 cm yr^{-1} from AD 1700–1940 (122 cm to 18 cm). Afterward, the sediment accumulation rate decreased to ca. 0.27 cm yr^{-1} from AD 1940 to the present (18–0 cm).

4.2. Palynological Results

In total, 118 pollen and 26 spore taxa were identified in the 40 samples from DK. The pollen and spores were well-preserved and the pollen concentration was high along the core (average 120,000 grains cm^{-3}). The bottom part (298–254 cm) showed a high pollen concentration (average 205,000 grains cm^{-3}). The pollen concentration then decreased from 251 to 110 cm (average 110,000 grains cm^{-3}), followed by a continuous decrease from 110 to 18 cm (average 97,000 grains cm^{-3}). Subsequently, the pollen concentration reached its lowest level in the upper part of the sediment core from 18–0 cm (average 64,000 grain cm^{-3}).

The pollen diagram displayed the relative abundance of dominant and essential pollen and spore taxa, grouped after their ecological affiliation within KSNP (i) submontane rainforest vegetation (SMF), representing the pollen of plants that are commonly found in submontane forest; (ii) disturbance/anthropogenic and open vegetation (AOF—herbs and pioneer trees), representing pollen produced by herbaceous and pioneering plants found in open areas or are growing fast after disturbance; (iii) ferns; and (iv) non-pollen palynomorphs (NPPs).

The pollen taxa were further calculated into the ratio SMF/AOF between submontane forest taxa (SMF) and disturbance/anthropogenic and opening vegetation (AOF). AOF vegetation mainly comprises Cyperaceae, Poaceae, *Mallotus/Macaranga*, Asteraceae, and *Trema*. On the other hand, SMF vegetation mainly include *Lithocarpus/Castanopsis*, *Ficus*, *Celtis*, *Bischofia*, *Alnus*, *Dacrycarpus*, Pinaceae, *Podocarpus*, Myrtaceae, and Moraceae/Urticaceae. The DK record can be divided into three zones according to the main changes in the palynological composition based on the cluster analysis of terrestrial pollen (CONISS) and the XRF scanning results (Figure 3).

4.2.1. Zone DK-1 (298–254 cm; Ca. AD 200–AD 500; 6 Samples)

In this zone, the SMF pollen taxa were dominant (79%), mainly represented by Moraceae/Urticaceae (30%) and *Elaeocarpus* (13%), followed by *Lithocarpus/Castanopsis* (3%), *Ficus* (3%), *Saurauia* (2%), *Celtis* (2%), Myrtaceae (2%), Dipterocarpaceae (1%), particularly with *Engelhardia* (2%) and *Ilex* (4%). The AOF pollen signal (20%) was already present at the beginning of the core, dominated by pioneer trees such as *Macaranga/Mallotus* (12%) and *Trema* (8%). All other taxa showed low relative abundance (<1%) along the whole record.
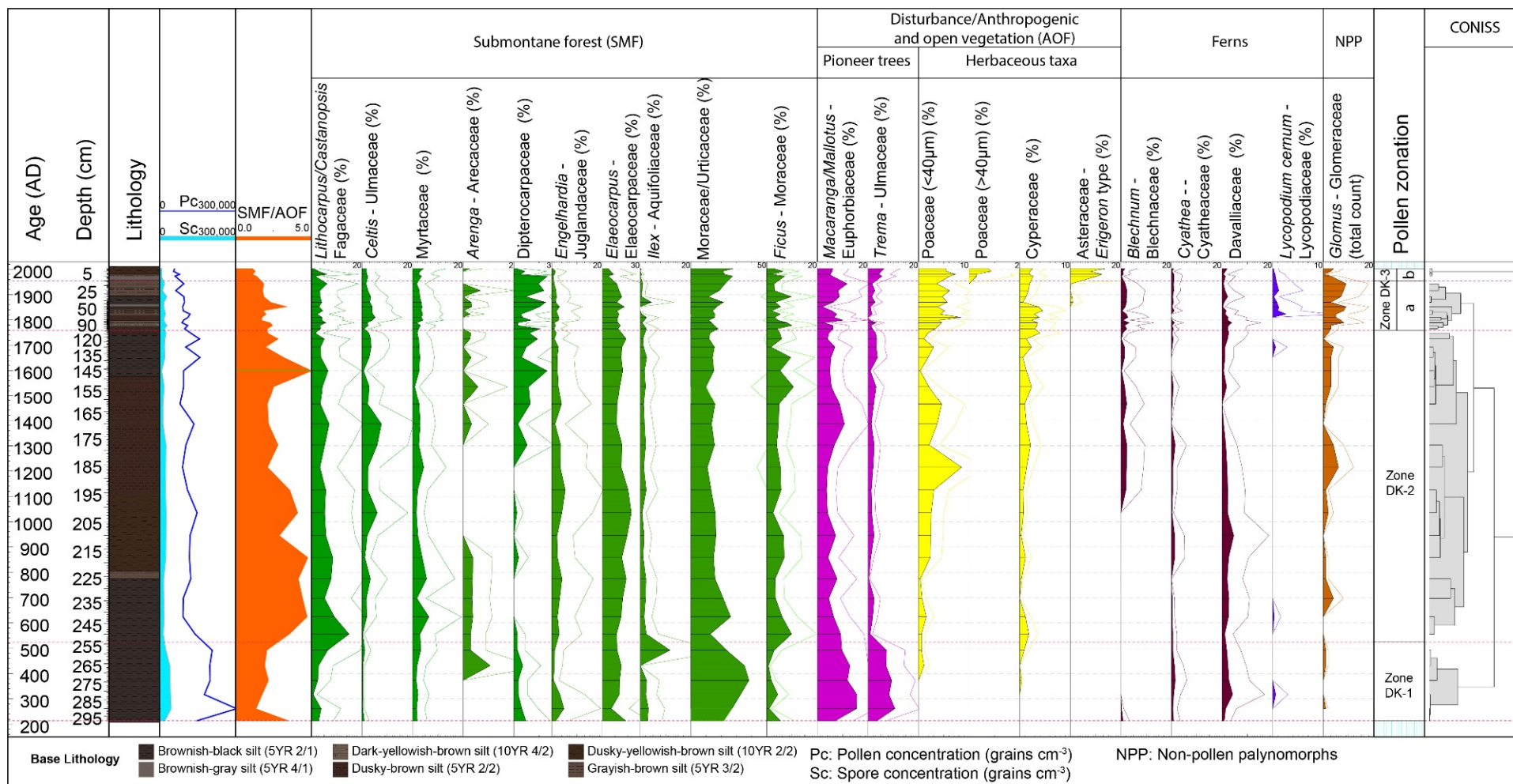
Figure 3. A palynological diagram of the DK core with lithology. The most important pollen and spore taxa are expressed as the percentages of the total sum of pollen (pollen taxa) and pollen plus spores (ferns). NPP-Glomus is expressed as the absolute total count.

4.2.2. Zone DK-2 (254–110 cm, Ca. AD 500–AD 1760; 18 Samples)

In this zone, the pollen of the SMF vegetation markedly increased (88%), especially *Elaeocarpus* (16%). Other taxa also increased including *Lithocarpus/Castanopsis* (6%), *Ficus* (6%), *Saurauia* (5%), *Engelhardia* (2.5%), *Bischofia* (3%), *Celtis* (4%), and Myrtaceae (3%). However, *Ilex* (2%) and Moraceae/Urticaceae (15%) decreased. The AOF pollen markedly decreased (12%) mainly due to the decrease in the pioneer taxa *Macaranga/Mallotus* (6%) and *Trema* (2%). There was an increase in small Poaceae (<40 μm) from >1% in zone DK-1 to 2% in this zone.

4.2.3. Zone DK-3 (110–0 cm, AD 1760–Present; 16 Samples)

This zone was further divided into two subzones according to marked changes in the pollen composition: Zone DK-3a (110–18cm, AD 1760–1940) and zone DK-3b (18–0 cm, AD 1940 to present). In zone DK-3a, the pollen of the SMF vegetation decreased (83%), led by the decrease in *Elaeocarpus* (13%), *Ficus* (5%), *Lithocarpus/Castanopsis* (4%), *Bischofia* (3%), and *Celtis* (2%), while Moraceae/Urticaceae (16%) and *Saurauia* (6%) increased. The AOF pollen strongly increased (16%) mainly due to *Mallotus/Macaranga* (7%), Cyperaceae, and small Poaceae (<40 μm), which increased 3% and 5%, respectively. In zone DK-3b, the sum of the SMF pollen continuously decreased (68%) with a reduction in *Elaeocarpus* (6%), *Lithocarpus/Castanopsis* (3%), *Saurauia* (3%), *Bischofia* (2%), and *Celtis* (1%) pollen, Moraceae/Urticaceae increased (24%) while *Ficus* remained at 5%. On the other hand, the AOF pollen increased (30%) including small Poaceae (6%), Asteraceae (11%), Cyperaceae (2%), *Trema* (5%), and *Mallotus/Macaranga* (6%). Poaceae with a grain size >40 μm were frequent in this subzone.

4.3. X-ray Fluorescence–Scanning Results

The X-ray fluorescence analysis scans the content of lithogenic elements in the sediment. The XRF scanning results showed about 23 elements along the core including siliciclastic elements such as Ti, Fe, K, Si, Zr, Zn, Cu, and Pb, and carbonate-derived elements such as Ca and Sr (Figure 4). In zone DK-1, the siliciclastic elements were dominated by Fe (average 6528 counts per second (cps)). Other elements were present in low values including Ti (485 cps), Zr (279 cps), K (49 cps), and Si (44 cps). In zone DK-2, the siliciclastic elements decreased, but were still dominated by Fe (4890 cps). Other elements were low and slightly decreased including Ti (303 cps), Zr (256 cps), K (48 cps), and Si (38 cps). In zone DK-3, the siliciclastic elements significantly increased, with Fe still being the most dominant element (6489 cps), followed by Ti (528 cps), Zr (408 cps), K (64 cps), and Si (52 cps). The carbonate-derived element Ca showed a decreasing trend along the core. In zone DK-1, the Ca concentration was about 366 cps. It then declined to 285 cps in zone DK-2 and decreased to 237 cps in zone DK-3. Another dominant carbonate element, Sr, stayed stable along the core with an average measurement of about 200 cps. The values of other elements including Cr, Al, Mn, Br, Rb, Pb, Ge, Ga, Ni, Cu, Zn, S, P, Cl, Ar, Y, Mo_{inc}, and Mo_{coh} were stable along the record.

Figure 4. The X-ray fluorescence scanning diagram for multiple elements measured in the DK core. Each element's value is expressed as counts per second (cps).

4.4. Macro-Charcoal and Fire Regime

In general, the macro-charcoal analysis resulted in a low charcoal signal, with few char-coal counts and a low concentration along the entire DK sediment core (minimum count = 0 and maximum count = 26). The macro-charcoal concentration registered low values along the whole core (minimum concentration = 0 and maximum concentration = 22 particles cm^{-3}). In total, eight fire peaks could be distinguished from the background signal. The global signal to noise index was rather low (1.6), possibly due to constantly low charcoal counts, causing only a few samples to fall above the threshold to be interpreted as a signal. Study-ing the local signal to noise index (SNI) in more detail, only four fire peaks fell above a SNI threshold of 3 and could be identified as potentially local fire signals (red cross, Figure 5a). The mean fire return interval (mFRI) was 245 with a mean fire frequency of about two peaks per 500 years (Figure 5b,c,e). In detail, zone DK-1 (298–254 cm; AD 200–500) showed a higher macro-charcoal concentration (average 5 particles cm^{-3}) and fire frequency (ca. 3 peaks per 500 year) than the following zone DK-2 (254–110 cm; AD 500–1760) with ca. 1 particles cm^{-3} and a fire frequency of two peaks per 500 years. In zone DK-3 (110–0 cm; AD 1760–present), the charcoal concentration increased again (ca. 4 particles cm^{-3}), coinciding with the highest fire frequency along the core (ca. 5 peaks per 500 years, Figure 5c).
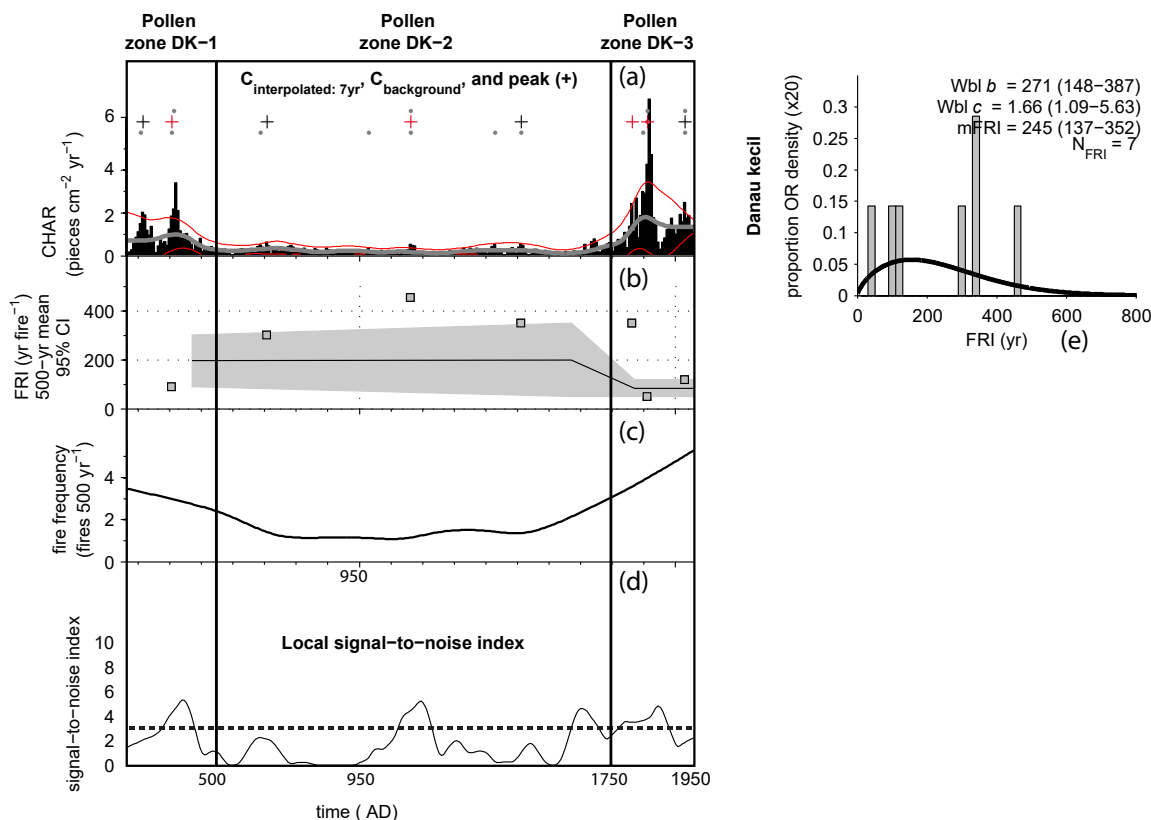

Figure 5. The reconstructed fire regime from the DK core was obtained by CharAnalysis (Higuera et al., 2009). (**a**) Raw charcoal counts were interpolated to 7 yr intervals ($C_{interpolated}$); reconstructed fire episode inferred fire frequency (fires 500 yr window) with a total of eight fire peaks (black crosses). (**b**) Corresponding fire frequency (500 yr window). (**c**) Corresponding mean fire frequency (500 yr window). (**d**) Local signal-noise index (SNI). (**e**) The mean fire return interval (mFRI) was 245 yrs.

4.5. Multivariate Statistical Results

Both PCA and DCA were performed on the square-root transformed data, however, the unimodular DCA showed a gradient length of 1.4 SD (<2.5 SD). Hence, a linear re-sponse model (PCA) was more appropriate. PCA was chosen to summarize the change

in palynological composition over time, as shown in Figure 6. Consequently, the PCA results indicate that 34% of the total variance can be explained by the first (19%) and second (15%) axes. PC1 aligns with the development stage of submontane forests with taxa such as *Lithocarpus/Castanopsis, Ilex, Elaeocarpus, Engelhardia*; PC2 likely coincides with secondary forest taxa including *Trema, Mallotus/Macaranga,* Moraceae/Urticaceae, and herbaceous taxa (Poaceae, Cyperaceae, Asteraceae).
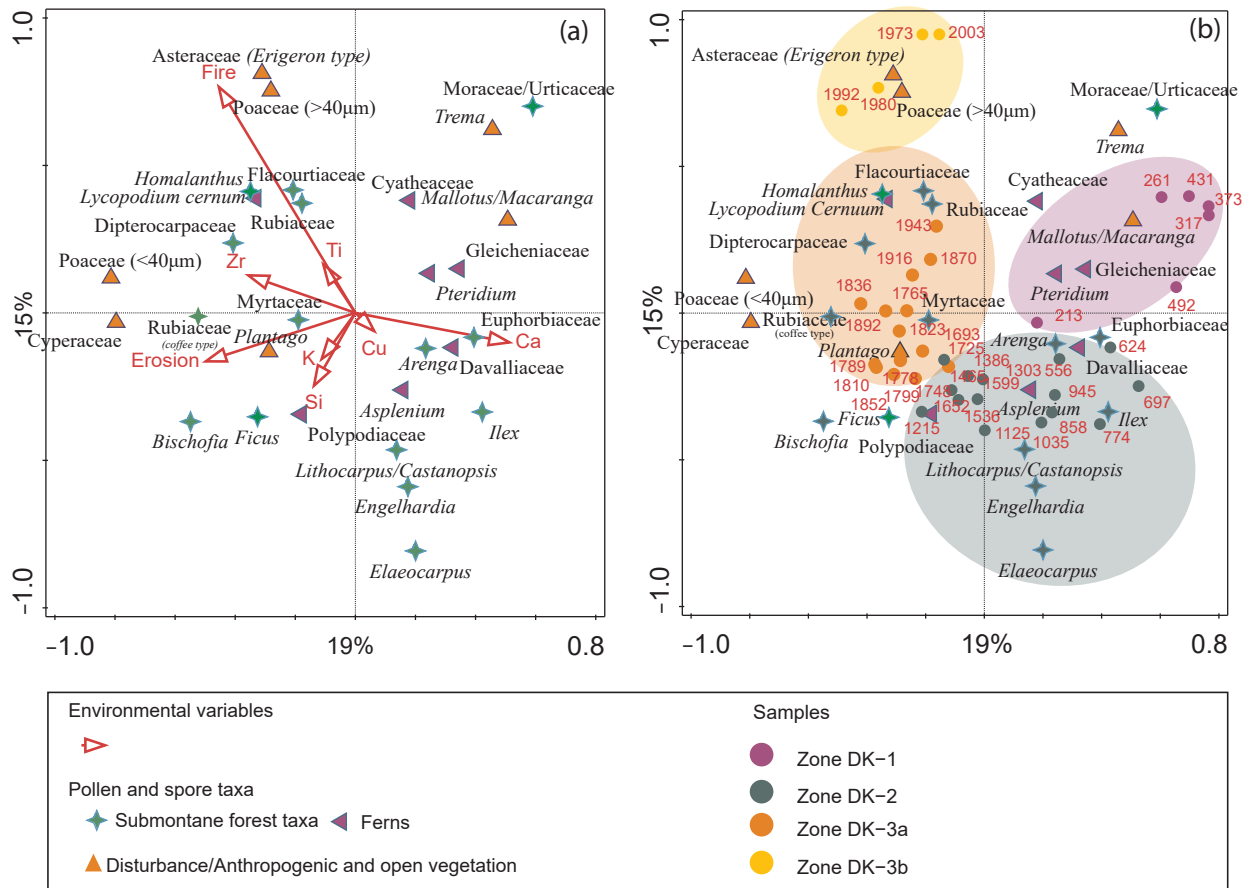
Figure 6. The PCA of the percentage data of identified pollen and spores. Supplementary environmental variables were the fire frequency obtained from CharAnalysis, the non-pollen palynomorph (*Glomus*) concentration for erosion, and the lithogenic elements (Ti, Si, K, Cu, Ca, Zr) obtained from the XRF analysis. The first two eigenvalues accounted for 34% of the total variance in composition (PC1: 19%, PC2: 15%). (**a**) Biplots show the representative pollen and spore taxa of each palynological group and the environmental variables driving the vegetation change. (**b**) Biplot species and samples showed a relationship between the sample and pollen and spore taxa of each zonation. Red numbers are the estimated age in AD of each sample.

The results from the RDA indicate that 67% of the variation can be explained by certain environmental variables, significantly defining changes in the pollen and spore composition. The simple effect model revealed the independent effects of individual environmental variables (Table 2a). The conditional effect model summarizes the conditional effect of each environmental variable after accounting for the effect of the variable enhancing explained variation (Table 2b). The results from both models showed that only fire and erosion significantly correlated with the variance in the taxa composition ($p < 0.005$ adjusted from the false discovery rate). The largest part of the variance for both models (13.5%) was explained by fire, while erosion simultaneously explained 6.9% and 7% for both the simple term effect and the conditional term effect, respectively.

Table 2. The results from the redundancy analysis (RDA).

(a) RDA-Simple Term Effects				(b) RDA-Conditional Term Effects			
Name	Explains (%)	Pseudo-F	*p*	Name	Explains (%)	Pseudo-F	*p*
Fire	13.5	5.9	0.002	Fire	13.5	5.9	0.002
Erosion	6.9	2.8	0.004	Erosion	7.0	3.2	0.002
Ca	6.1	2.5	0.006	Ca	3.8	1.8	0.016
Zr	4.6	1.8	0.018	Cu	3.0	1.4	0.032
Ti	3.4	1.3	0.164	Ti	2.6	1.2	0.158
Cu	3.1	1.2	0.23	K	2.7	1.3	0.128
Si	2.8	1.1	0.292	Si	2.0	1.0	0.494
K	2.2	0.8	0.642	Zr	1.8	0.9	0.718

5. Discussion

5.1. Forest Disturbance and Anthropogenic History

5.1.1. Period 1–Forest Opening and Initial Cultivation (AD 200–500, Pollen Zone DK-1)

At the beginning of DK-1, the palynological composition indicates a submontane rainforest surrounding DK with taxa such as Myrtaceae, Dipterocarpaceae, *Elaeocarpus*, and *Ilex* possibly forming part of the canopy [15]. The submontane forest signal is complemented by fast growing pioneer and secondary forest taxa such as *Trema*, *Mallotus*, and *Macaranga*. This secondary forest signal, coinciding with the presence of *Engelhardia* as a prolific and fast-growing tree, indicates a period of succession after disturbance [55].

Indeed, our results (Figure 3) show an establishment of secondary forest, dominated by pioneer trees such as *Trema*, *Mallotus*, *Macaranga*, and Moraceae/Urticaceae since AD 200. In general, the *Trema*, *Mallotus*, and *Macaranga* communities are widely distributed in Kerinci as pioneer trees after disturbance [18,56]. The families of Moraceae and Urticaceae are also part of this natural succession as they include many fast-growing species. Urticaceae species are important components in forest regeneration [57], generally found at the first stage of colonization in the undergrowth of agroforestry systems and secondary forest [15,58]. Moraceae are predominantly found in both primary and secondary forests in Kerinci [15]. These interpretations were also confirmed by the PCA (Figure 6), showing that Moraceae/Urticaceae were positively correlated with the pioneer trees *Trema* and *Mallotus/Macaranga*. Indicators of forest opening and disturbance, moreover, seem to correlate with increasing indicators of soil erosion, as displayed by an increasing abundance in Ti, Si, Fe, Zr, and K (Figure 4). Perhaps canopy openness led to increased surface runoff, and consequently erosional processes [54]. Human activities probably caused forest opening, and climate may have also played a role (see Section 5.2).

A potential indication of agroforestry systems around DK is the occurrence and increase in *Arenga* since 400 AD. Humans probably cultivated *Arenga* (sugar palm) as a source of sugar and its fiber [18,59,60]. Our study showed similar results to Morley [18] and Flenley [61] in the Padang Lake area (about 5 km from the study site) with a rapid expansion of pioneer trees (e.g., *Macaranga*, *Trema*) about 2000 BC as well as the occurrence of *Arenga*, which was perhaps cultivated since AD 50. According to δ18O stable isotope ratios obtained from the Tangga cave (Figure 1a and Figure 8; [19]), the development of *Arenga* in this period aligns with drier conditions from AD 350–660 (see Section 5.2). However, *Arenga* trees develop best under high rainfall conditions [62]. Perhaps the occurrence of *Arenga* in the DK record, despite drier conditions during this period, indicates that it was planted in closer proximity to the lake for sufficient irrigation. There is little archeological information during this period, except that the people who settled in the area conducted agriculture [29]. In this pollen record, the decline in submontane forest components such as *Lithocarpus/Castanopsis*, Dipterocarpaceae, *Bischofia*, and the growing *Arenga* sugar palm suggests that the forest has possibly been exploited for timber production and agricultural practices, possibly indicating the intensification of human activities in the forest. On the

other hand, climate change may also affect the decline in a submontane forest signal (climatic conditions are discussed in Section 5.2)

In addition, the CharAnalysis results showed higher fire frequencies, with one fire peak (SNI threshold > 3), indicating that fires might be associated with forest opening. This is reflected in Figure 7; within four explanatory variables, only AOF vegetation had a significant effect on the fire frequency with a sharp positive slope, indicating that the fire frequency increased after forest disturbance (Figure 7a). In contrast, a higher proportion of submontane vegetation (SMF/AOF) contributes to a lower fire frequency, as shown by the curve (Figure 7b). The residual model between the fire frequency and paleo-precipitation record from Tangga Cave [19] did not show a meaningful correlation (Figure 7c). This finding suggests that the forest opening and closed canopy forest may play a more important role for the occurrence of fires than climatic factors. Consequently, the probability of fire appearing in the open forest will be higher than in a closed canopy forest. However, this interpretation should be handled with care as the open forest signal coincides with an increase in erosion indicators. While forest opening and increased surface runoff may have led to erosional sediment input into the lake, this additional sediment influx may lead to false charcoal peaks (e.g., [63]). On the other hand, the results of the PCA (Figure 6) only displayed a similar direction in the environmental variable "fire" and "Ti", while "erosion" (*Glomus*) and other siliciclastic elements such as "Si" or "Fe" did not align with fire and/or go into the direction of AOF.
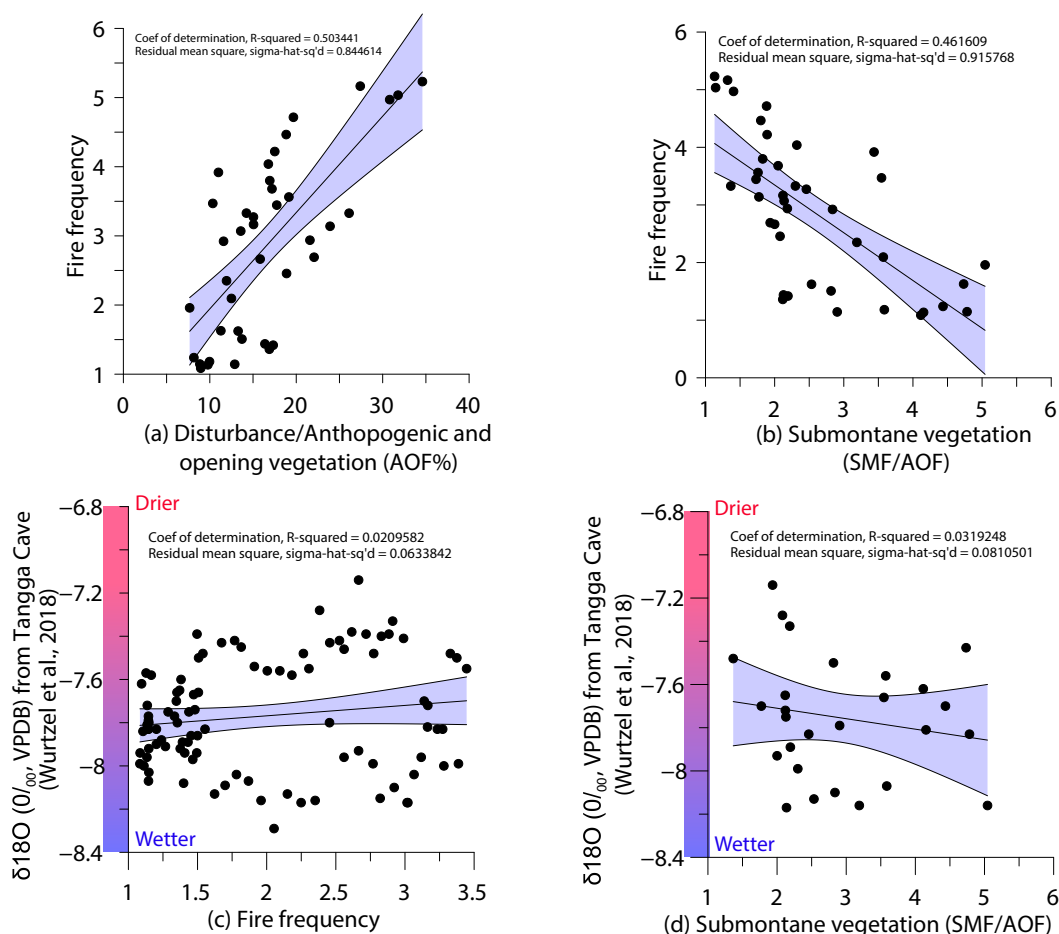
Figure 7. Fitted simple linear regression to model the relationship between (**a**) fire frequency vs. disturbance/anthropogenic and opening vegetation (AOF%). (**b**) Fire frequency vs. submontane vegetation (SMF/AOF). (**c**) Fire frequency vs. paleo-precipitation record. (**d**) Vegetation paleo-precipitation record. Variables used: Fire frequency from CharAnalysis [46], paleo-precipitation data from Tangga Cave [19], and vegetation from palynological data in percentage.

5.1.2. Period 2–Submontane Forest Regeneration and Initial Agroforestry (AD 500–1760, Pollen Zone DK-2)

This period is marked by the regeneration of the submontane forest, as shown by an increase in *Lithocarpus/Castanopsis, Celtis, Ficus*, Myrtaceae, *Bischofia*, and other taxa, while pioneer trees such as *Mallotus/Macaranga* and *Trema* are decreasing. On the other hand, an increase in Poaceae pollen indicates more open forest areas, facilitating the growth of herbaceous taxa [28]. Around the lake, *Elaeocarpus* remained stable, while *Ilex* showed a decreasing trend after reaching its maximum at ca. AD 430. Possibly, this indicates a change in the water level, causing less suitable conditions for *Ilex* to grow along the lake shore. The regrowth and compositional change in the submontane forest is possibly driven by high rainfall conditions, perhaps causing a change in the water level (see Section 5.2).

Regarding human activities, the continuous occurrence of *Arenga* since AD 500 can be traced from the pollen record (Figure 3), implying that humans have continuously planted sugar palm in proximity to the lake, suggesting the establishment of traditional agroforestry systems around Danau Kecil. Traditional agroforestry relied on forest gaps, enabling the planting of crops without interrupting natural forest recovery [59]. Forest regeneration, together with cash crops (*Arenga*), suggests a possibly intensive integration of forest vegetation and stable crops [60]. This agroforestry system was common in Indonesia, where agriculture was integrated in natural forest areas to form a mosaic of natural rainforest and agro-forestry systems [15]. However, starting from ca. AD 860, *Arenga* decreased and eventually almost disappeared. This dynamic suggests that the area around the lake was somehow not suitable or convenient for growing *Arenga*.

In the upper part of DK-2 (ca. AD 1300), Dipterocarpaceae strongly increased. This was followed by the reoccurrence of Arenga, ca. AD 1400, albeit in low frequencies. Perhaps the reestablishment of *Arenga* was again related to agricultural activities, reintroducing *Arenga* as a crop in the region. However, *Arenga* pollen only reached a low abundance (<2%). It is difficult to differentiate whether the synchronous increase in Dipterocarpaceae pollen is related to a shift toward suitable environmental conditions and/or human influence (plantation or protection). However, considering that the Srivijaya–Melayu Kingdom occupied most of the Jambi lowlands as well as south Sumatra between the 7th–14th centuries AD, it is possible that an increase in Dipterocarpaceae pollen is related to dipterocarp agroforestry and/or protection efforts, especially since Dipterocarpaceae formed a valuable source of timber and damar resin. The Srivijaya–Melayu realm was predominantly a maritime kingdom and coastal trading center. With the majority of trading being carried out by sea, available ships and shipbuilding were an essential component of the kingdom's success. Notably, both timber and resin from Dipterocarpaceae was used domestically for shipbuilding, where resin was majorly used for varnishes and boat caulking [64–66]. In this context, the high increase in Dipterocarpaceae could be interpreted as a signal of dipterocarp agroforestry, where Dipterocarpaceae were intermixed in a natural secondary forest. This is an interesting example of sustainable and complex past agroforestry in Sumatra, where the garden is ecologically part of the forest, but managed as an agricultural system [67]. Anyhow, it is just as likely that climatic and/or site-specific conditions changed in favor of both the Dipterocarpaceae and *Arenga* taxa, promoting their expansion. Moreover, between AD 900 and 1300, the population within the area of Kerinci territory possibly expanded into the proximity of DK, as indicated by archeological finds such as burial jars, a megalithic tomb, and a processed stone, formerly connected to a house of a small-scale settlement (Bonatz et al., 2009; Tjoa-Bonatz, 2009). As they were found in close proximity to DK, these remains suggest a nearby settlement and would explain human activity such as forest use or plantations in the surrounding submontane area.

5.1.3. Period 3–Intensification and Permanent Agroforestry System (AD 1760 to Present, Pollen Zone DK-3)

DK-3 is characterized by a high abundance of Dipterocarpaceae pollen, while other rainforest taxa such as *Lithocarpus/Castanopsis, Bischofia*, and *Elaeocarpus* decreased (Figure 3).

The increasing abundance of Dipterocarpaceae align well with historical reports of permanent Dipterocarpaceae plantations for resin production [15,68,69]. In 1783, a British historian visited South Sumatra and noticed that people had planted *Shorea javanica* trees for resin production [70]. Since AD 1783, damar resin production has been recognized as an important component of Sumatra's economy and become one of Sumatra's most important international commodities [71]. Before the introduction of petrochemical resins in 1945, damar resin was a component of various industrial substances (e.g., industrial varnishes, paint [66]). Damar resin was first exported to America and Europe in the 1830s [72]. Later, the export volume of resin from Sumatra exceeded 280 tons in AD 1843 [70]. Therefore, an increase of Dipterocarpaceae pollen in the DK record since ca. AD 1820 may indicate human made plantations of Dipterocarpaceae for damar resin extraction. However, suitable environmental conditions may again play a role in this development.

Furthermore, in DK-3, Poaceae started to increase and remained stable afterward. Cyperaceae also increased and slightly decreased in the mid 1800s. This suggests increasing areas of forest opening, perhaps as a consequence of intensified agriculture. A high peak magnitude and two distinct fire peaks with a high signal-to-noise index (Figure 5) would substantiate the assumption of increasing agricultural activities, perhaps including slash and burn practices. This coincides with Bonatz [5], stating that during the Dutch occupation, various settlements by the hill sites were forced to move to the valley to promote the expansion of rice cultivation as well as the cultivation of cash crops (e.g., coffee, cinnamon; [68]). In the same period around ca. AD 1940, large Poaceae pollen (>40 µm) notably also increased, together with an increase in Asteraceae. Large Poaceae pollen, originating from cultivated grasses, could indicate rice cultivation in flat areas around DK. Compared to other records of early rice cultivation in Kerinci, the plantation of rice around DK started rather late. This might be due to the fact that the landscape around DK is rather steep and therefore not ideal for rice cultivation. Anyhow, the cooccurrence of Asteraceae (*Erigeron* type) supports the assumption of rice plantations around DK. Asteraceae such as *Erigeron sumatrensis* often grow as weeds in rice fields as well as in recently burned areas, indicating strong disturbance [73].

The increased siliciclastic input of Si, Ti, Fe, K, and Zr (Figure 4) indicates stronger mechanical erosion related to intensive surface runoff and sediment transportation within this period [54]. The soil exposure, related to human activities in this period, might have caused serious soil erosion and sediment deposition into the lake. The increase in *Glomus* fragments (Figure 3) further confirms intensive soil erosion [74]. As above-mentioned, it should be considered that an increased signal of erosion correlating with an increased fire signal might indicate the formation of false charcoal peaks.

5.2. Role of Climate on the Vegetation Dynamics

Climate variability is another important factor driving vegetation change in Sumatra aside from anthropogenic activities (e.g., [69,75]). According to the δ18O record from Tangga Cave [19], precipitation in West Sumatra has fluctuated between drier and wetter climatic conditions since AD 200 (Figure 8). Between ca. AD 350–660 and AD 1100–1460, Tangga Cave showed the maximum δ18O values, indicating the driest period in Sumatra [19,76]. On the other hand, the decrease in δ18O values in the period from AD 660 to 1100 and AD 1460–1750 suggests an increase in precipitation in Sumatra [19,76]. The increase and decrease in precipitation somehow affected the development and degradation of forests, inferring the change in vegetation (SMF/AOF) as well as *Lithocarpus/Castanopsis, Ilex, Engelhardia*, and herbaceous taxa can be used as climatic indicators in our study (Figure 8).
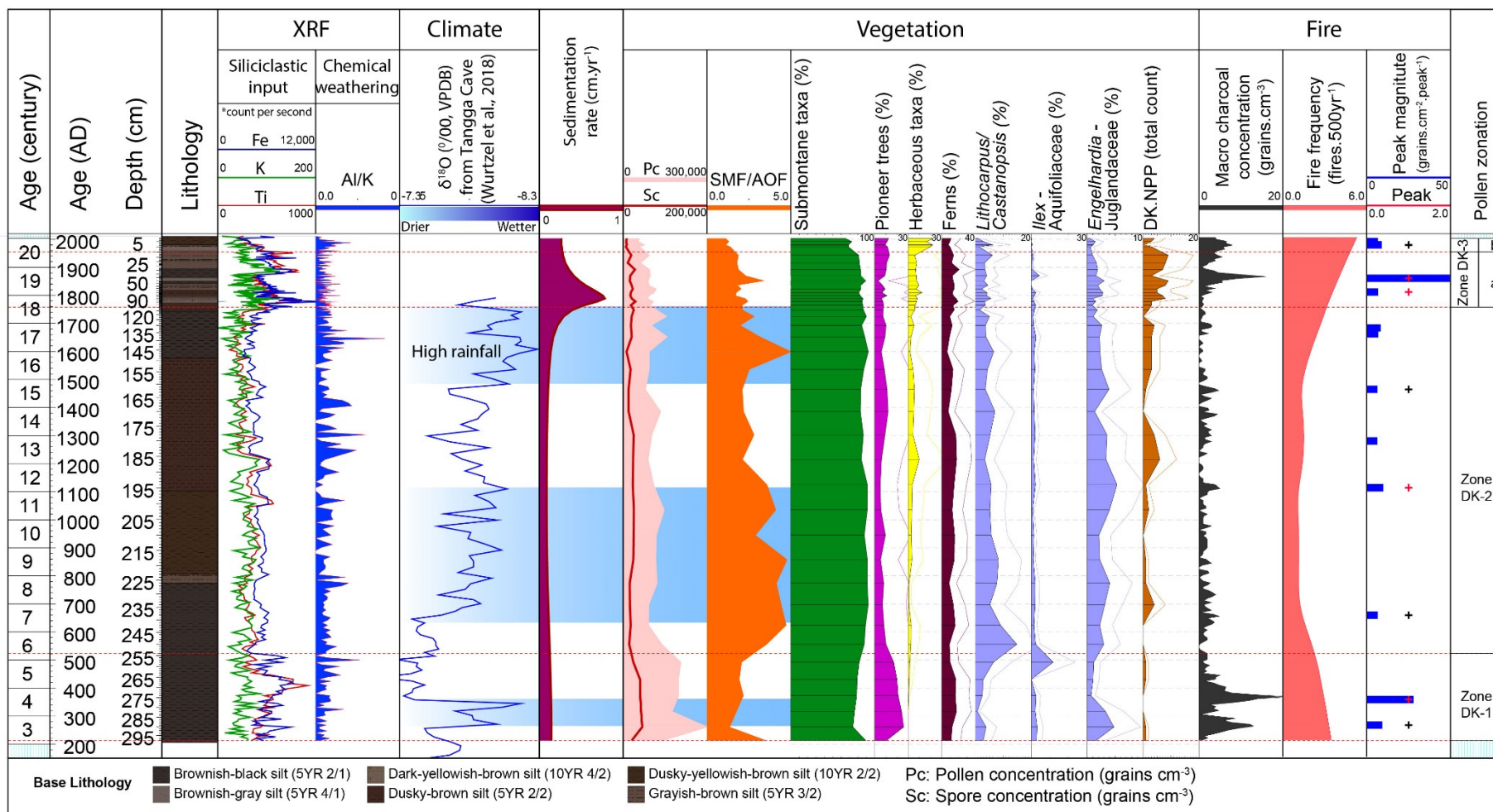
Figure 8. A palynological diagram of the DK core represents the total sum pollen and spore taxa for each ecological group, non-pollen palynomorph concentrations (*Glomus*), CharAnalysis results (macro charcoal concentration, fire peaks (red cross: fire peaks with a high SNI >3), peak magnitude, and fire frequency), XRF data (Ti, K, Fe, AI/K) and the climate data (paleo-precipitation record from Tangga Cave [19]).

Our pollen record (Figure 8) showed the high ratio SMF/AOF in three periods: AD 200–350, AD 660–1100, and AD 1460–1750. This coincides with the low value of δ18O, indicating a period of high precipitation [19]. The growth of *Engelhardia, Elaeocarpus,* and the high ratio of SMF/AOF seems to correspond to the increase in precipitation. It is likely that 200 years is the average time for forests to recover in favorable climatic conditions. In contrast, the high value of δ18O from AD 350 to 660 and AD 1100–1460 indicates a dry period [19], accompanied by an amplification in ENSO events [76,77]. This coincides with a decrease in SMF/AOF in the DK record (Figure 8). In particular, the driest period of the record between AD 350 and 650 was associated with a peak of *Lithocarpus/Castanopsis* and *Ilex* in the DK profile at AD 550. This result is consistent with the study by Zeist, et al. [78] in Seitu Gunung and Telaga Patengan in West Java, suggesting that an increase in *Lithocarpus/Castanopsis* reflects a drier climate. Moreover, the peak of *Ilex* may suggest more suitable conditions for *Ilex* along the lake shore, perhaps due to a lower water level, which in turn allowed for more area to be populated, as the lake is usually surrounded by steeper slopes. This explanation seems reasonable when combined with the δ18O data from Tangga Cave [19] in which the dry season and reduced rainfall may have led to a decrease in water level. Furthermore, as local burning can also be caused by wildfires, a fire peak with a high signal-to-noise index could also reflect the wildfires during the dry season.

6. Summary and Conclusions

The multi-proxy analyses from the Danau Kecil (DK) sediment core allowed for the reconstruction of the vegetation and human impact in the Kerinci area since AD 200. The forest dynamics can be categorized into three periods, displaying the progression from forest opening to agriculture around DK. Initially, forest logging and landscape opening for possible *Arenga* sugar palm cultivation may have caused a decrease in submontane forest and the expansion of pioneer trees at the beginning of AD 200–500. Human activities are likely to be the main factor for the reduction in submontane forests, leading to enhanced soil erosion. The second period from AD 500 to 1760 was marked by the regeneration of the submontane forest with climax species such as *Bischofia, Celtis*, and *Lithocarpus/Castanopsis*. Dipterocarpaceae increased strongly after AD 1300, followed by *Arenga* ca. AD 1400, perhaps indicating efforts to manage the forest again with profitable crops such as sugar palm (*Arenga pinnata*) and Dipterocarpaceae for timber and resin extraction, supported by suitable natural conditions. Within this period, high precipitation possibly played the main factor contributing to the regrowth of the submontane forest. The last period from AD 1760 showed a decrease in the submontane forest taxa while Dipterocarpaceae were still well-developed. This could indicate the development of forest cultivation and expansion of the agricultural area, possibly through rice cultivation, into the flat areas of the valley. Agroforestry became more permanent by replacing natural vegetation in the forest with valuable trees such as Dipterocarpaceae. Furthermore, the increase in human activities and the expansion of farming probably explains the increased soil erosion.

This study may contain a few uncertainties. Aside from the limitations of paleoecological reconstruction (e.g., pollen preservation, pollen source area, sample resolution etc.), we expect erosion events to have influenced the upper and lower part of the core, possibly causing irregular sediment input. This may have possibly led to inconsistent C14 dates of the organic bulk sediment and false charcoal peaks. Second, the relationship between past precipitation and vegetation transpired to be rather unclear, affirming the need for further studies on this topic within the area. The incorporation of further climatic variables that affect the phenology such as regional precipitation variability and temperature could help to better distinguish climate induced changes in the vegetation [79,80]. Finally, archeological evidence and records are sparse in the area, only allowing for limited assumptions on past human–forest interactions. As paleoecological studies within the KSNP are also limited, there are only a few comparative records. More studies are required to understand the paleoecological background, forest dynamics, and past land use of the KSNP.

Despite this, in our results, the regeneration of the submontane forest took place about 200–300 years after disturbance. Therefore, 200 years is likely to be an efficient time to recover/regenerate the vegetation. Furthermore, our results indicate that a higher fire frequency can be significantly explained by forest opening. Therefore, maintaining a closed canopy should be a priority to reduce the wildfire risk, caused either by humans and/or natural conditions. In conclusion, we emphasize the need to preserve a closed canopy and to uphold forest restoration concession licenses over at least 200 years. Furthermore, well-designed residential and agricultural areas, integrated close to the natural forest, should also be considered.

References

1. Ministry of Agriculture. *Agricultural Development in Indonesia 1996–2000*; Ministry of Agriculture, Republic of Indonesia: Jakarta, Indonesia, 2001.
2. Maloney, B.K. Possilble Early Dry-land and Wet-land Rice Cultivation in Highland North Sumatra. *Asian Perspect.* **1996**, *35*, 165–192.
3. Bellwood, P. *Prehistory of the Indo-Malaysian Archipelago (Revised Edition)*; ANU Press: Canberra, Australia, 2007.
4. Setyaningsih, C.; Behling, H.; Saad, A.; Shumilovskikh, L.; Sabiham, S.; Biagioni, S. First palaeoecological evidence of buffalo husbandry and rice cultivation in the Kerinci Seblat National Park in Sumatra, Indonesia. *Veg. Hist. Archaeobotany* **2019**, *28*, 591–606. [CrossRef]
5. Bonatz, D. A Highland Perspective on the Archaeology and Settlement History of Sumatra. *Archipel* **2012**, *84*, 35–81. [CrossRef]
6. Dudgeon, D. Multiple threats imperil freshwater biodiversity in the Anthropocene. *Curr. Biol.* **2019**, *29*, R960–R967. [CrossRef]
7. Hlásny, T.; Krokene, P.; Liebhold, A.; Montagné-Huck, C.; Müller, J.; Qin, H.; Raffa, K.; Schelhaas, M.-J.; Seidl, R.; Svoboda, M.; et al. Living with bark beetles: Impacts, outlook and management options. *Sci. Policy* **2019**, *8*, 1–50. [CrossRef]
8. Nikonovas, T.; Spessa, A.; Doerr, S.H.; Clay, G.D.; Mezbahuddin, S. Near-complete loss of fire-resistant primary tropical forest cover in Sumatra and Kalimantan. *Commun. Earth Environ.* **2020**, *1*, 65. [CrossRef]
9. Tacconi, L. *Fire in Indonesia*; CIFOR Occasional Paper; Center for International Forestry Research: Bogor, Indonesia, 2003; Volume 38.
10. Vetrita, Y.; Cochrane, M.A. Fire Frequency and Related Land-Use and Land-Cover Changes in Indonesia's Peatlands. *Remote Sens.* **2019**, *12*, 5. [CrossRef]

11. Anderson, I.P.; Imanda, I.D.; Muhnandar. *Vegetation Fires in Sumatra, Indonesia: A first Look at Vegetation Indices and Soil Dryness in Relation to Fire Occurrence*; European Union Ministry of Forestry and Estate Crops, Forest Fire Prevention and Control Project: Palembang, Indonesia, 1999.

12. Nicolas, M.V.J.; Beebe, G.S. *Fire Management in the Logging Concessions and Plantation Forests of Indonesia*; European Union German Agency for Techical Cooperation, Ministry of Forestry and Estate Crops: Palembang, Indonesia, 1999.

13. Bowen, M.R.; Bompard, J.M.; Anderson, I.P.; Guizol, P.; Gouyon, A. *Anthropogenic Fires in Indonesia: A View from Sumatra, Preprint from Forest Fires and Regional Haze in South East Asia*; Nova Science: New York, NY, USA, 2001.

14. Fernandes, K.; Verchot, L.; Baethgen, W.; Gutierrenz-Velez, V.; Pinedo-Vasquez, M.; Maritus, C. Heightened fire probability in Indonesia in non-drought conditions: The effect of increasing temperatures. *Environ. Res. Lett.* **2017**, *12*, 054002. [CrossRef]

15. Laumonier, Y. *The Vegetation and Physiography of Sumatra*; Kluwer Academic: London, UK, 1997; Volume 12, p. 233.

16. Whitten, T.; Damanik, S.J. *The Ecology of Sumatra*; Periplus Editions (HK) Limited: Singapore, 2000.

17. Bramley, G.; Pennington, R.; Zakaria, R.; Tjitrosoedirdjo, S.R.I.; Cronk, Q. Assembly of tropical plant diversity on a local scale: Cyrtandra (Gesneriaceae) on Mount Kerinci, Sumatra. *Biol. J. Linn. Soc. Biol. J. Linn. Soc. Blackwell Sci.* **2004**, *81*, 49–62. [CrossRef]

18. Morley, R.J. A Palaeoecological Interpretation of a 10,000 Year Pollen Record from Danau Padang, Central Sumatra, Indonesia. *J. Biogeogr.* **1982**, *9*, 151–190. [CrossRef]

19. Wurtzel, J.B.; Abram, N.J.; Lewis, S.C.; Bajo, P.; Hellstrom, J.C.; Troitzsch, U.; Heslop, D. Tropical Indo-Pacific hydroclimate response to North Atlantic forcing during the last deglaciation as recorded by a speleothem from Sumatra, Indonesia. *Earth Planet. Sci. Lett.* **2018**, *492*, 264–278. [CrossRef]

20. Aziz, F.A. The Jar burial site of Lolo Gedang, Southwest of Kerinci Lake, Jambi. *Amerta J. Penelit. Dan Pengemb. Arkeol.* **2011**, *29*, 63–73.

21. Global Volcanism Program. Volcanoes of the World (VOTW) Database Information 2013, v. 4.10.2. Available online: https://volcano.si.edu/volcanolist_holocene.cfm (accessed on 24 August 2021).

22. Köppen, W. Versuch einer Klassifikation der Klimate, vorzugsweise nach ihren Beziehungen zur Pflanzenwelt. *Geogr. Z.* **1900**, *6*, 593–611.

23. Kottek, M.; Grieser, J.; Beck, C.; Rudolf, B.; Rubel, F. World Map of the Köppen-Geiger Climate Classification Updated. *Meteorol. Z.* **2006**, *15*, 259–263. [CrossRef]

24. Philander, S.G.H. El Niño, La Niña, and the Southern Oscillation. In *International Geophysics Series*; Holton, J., Dmowska, R., Eds.; Academic Press: New York, NY, USA, 1990; p. 289.

25. Cane, M.A. The evolution of El Niño, past and future. *Earth Planet. Sci. Lett.* **2005**, *230*, 227–240. [CrossRef]

26. Webster, P.J.; Moore, A.M.; Loschnigg, J.P.; Leben, R.R. Coupled ocean–atmosphere dynamics in the Indian Ocean during 1997–98. *Nature* **1999**, *401*, 356–360. [CrossRef]

27. Fick, S.E.; Hijmans, R.J. WorldClim 2: New 1-km spatial resolution climate surfaces for global land areas. *Int. J. Climatol.* **2017**, *37*, 4302–4315. [CrossRef]

28. Flenley, J.R.; Butler, K. Evidence for continued disturbance of upland rain forest in Sumatra for the last 7000 years of an 11,000 year record. *Palaeogeogr. Palaeoclimatol. Palaeoecol.* **2001**, *171*, 289–305. [CrossRef]

29. Klamer, M. The dispersal of Austronesian languages in Island South East Asia: Current findings and debates. *Lang. Linguist. Compass* **2019**, *13*, e12325. [CrossRef]

30. Simanjuntak, T. The Western Route Migration: A Second Probable Neolithic Diffusion to Indonesia. In *New Perspectives in Southeast Asian and Pacific Prehistory*; Piper, P.J., Matsumura, H., Bulbeck, D., Eds.; ANU Press: Canberra, Australia, 2017; pp. 201–211.

31. Harrison, T. A history of prehistory. *SMJ Sarawk Mus. J.* **1958**, *8*, 549–595.

32. Widianto, H. The Dawn of Humanity in Sumatra: Arrival and Dispersal from the Human Remains Perspective. In *From Distant Tales: Archaeology and Ethnohistory in the Highlands of Sumatra*; Bonatz, D., Miksic, J., Neidel, J.D., Tjoa-Bonatz, M.L., Eds.; Cambridge Scholar Publishing: Newcastle upon Tyne, UK, 2009.

33. Bonatz, D.; Neidel, J.D.; Tjoa-Bonatz, M.L. The megalithic complex of highland Jambi: An archaeological perspective. *Bijdr. tot taal-, land- Volkenkd./J. Humanit. Soc. Sci. Southeast Asia* **2008**, *162*, 490–522. [CrossRef]

34. Zervas, D.; Nichols, G.J.; Hall, R.; Smyth, H.R.; Lüthje, C.; Murtagh, F. SedLog: A shareware program for drawing graphic logs and log data manipulation. *Comput. Geosci.* **2009**, *35*, 2151–2159. [CrossRef]

35. Hogg, A.G.; Hua, Q.; Blackwell, P.G.; Niu, M.; Buck, C.E.; Guilderson, T.P.; Heaton, T.J.; Palmer, J.G.; Reimer, P.J.; Reimer, R.W.; et al. SHCal13 Southern Hemisphere Calibration, 0–50,000 Years cal BP. *Radiocarbon* **2013**, *55*, 1889–1903. [CrossRef]

36. Livingstone, D.A. A lightweight piston sampler for lake deposits. *Ecology* **1955**, *36*, 137–139. [CrossRef]

37. Blaauw, M. Methods and code for 'classical' age-modelling of radiocarbon sequences. *Quat. Geochronol.* **2010**, *5*, 512–518. [CrossRef]

38. R Core Team. *R: A Language and Environment for Statistical Computing*; R Foundation for Statistical Computing: Vienna, Austria, 2018.

39. Faegri, K.; Iversen, J. *Textbook of Pollen Analysis*, 4th ed.; Faegri, K., Kaland, P.E., Krzywinski, K., Eds.; John Wiley & Sons: London, UK, 1989.

40. Stockmarr, J. Tablets with Spores used in Absolute Pollen Analysis. *Pollen Et Spores* **1971**, *13*, 615–621.

41. *Stratabugs Biostratigraphic Data Management Software*; Stratadata: Pluckley, UK, 2014; Available online: https://www.stratadata.co.uk/ (accessed on 24 August 2021).

42. Grimm, E. CONISS: A FORTRAN 77 program for stratigraphically constrained cluster analysis by the method of incremental sum of squares. *Comput. Geosci.* **1987**, *13*, 13–35. [CrossRef]
43. Stevenson, J.; Haberle, S. *Macro Charcoal Analysis: A Modified Technique Used by the Department of Archaeology and Natural History*; Australian National University (ANU): Canberra, Australia, 2005.
44. Clark, J.S.; Lynch, J.; Stocks, B.J.; Goldammer, J.G. Relationships between charcoal particles in air and sediments in west-central Siberia. *Holocene* **1998**, *8*, 19–29. [CrossRef]
45. Carcaillet, C.; Bouvier, M.; Fréchette, B.; Larouche, A.C.; Richard, P.J.H. Comparison of pollen-slide and sieving methods in lacustrine charcoal analyses for local and regional fire history. *Holocene* **2001**, *11*, 467–476. [CrossRef]
46. Higuera, P.E.; Brubaker, L.B.; Anderson, P.M.; Hu, F.S.; Brown, T.A. Vegetation mediated the impacts of postglacial climate change on fire regimes in the south-central Brooks Range, Alaska. *Ecol. Monogr.* **2009**, *79*, 201–219. [CrossRef]
47. Lo, F.-L.; Chen, H.-F.; Fang, J.-N. Discussion of Suitable Chemical Weathering Proxies in Sediments by Comparing the Dissolution Rates of Minerals in Different Rocks. *J. Geol.* **2016**, *125*, 83–99. [CrossRef]
48. Profe, J. *X-ray Fluorescence Scanning of Discrete Samples—A New Tool for the Geochemical Characterization of Loess-Paleosol Sequences*; University of Bremen: Bremen, Germany, 2018.
49. Huang, C.; Kong, D.; Chen, F.; Hu, J.; Wang, P.; Lin, J. Multi—Proxy Reconstructions of Climate Change and Human Impacts Over the Past 7000 Years From an Archive of Continental Shelf Sediments off Eastern Hainan Island, China. *Front. Earth Sci.* **2021**, *9*, 478. [CrossRef]
50. Nesbitt, H.W.; Young, G.M. Early Proterozoic climates and plate motions inferred from major element chemistry of lutites. *Nature* **1982**, *299*, 715–717. [CrossRef]
51. Simpson, G.; Birks, H. *Statistical Learning in Palaeolimnology*; Springer: Berlin/Heidelberg, Germany, 2012; Volume 5, pp. 249–327.
52. Šmilauer, P.; Lepš, J. *Multivariate Analysis of Ecological Data Using CANOCO 5*, 2nd ed.; Cambridge University Press: Cambridge, UK, 2014.
53. Kylander, M.E.; Ampel, L.; Wohlfarth, B.; Veres, D. High-resolution X-ray fluorescence core scanning analysis of Les Echets (France) sedimentary sequence: New insights from chemical proxies. *J. Quat. Sci.* **2011**, *26*, 109–117. [CrossRef]
54. Davies, S.J.; Lamb, H.F.; Roberts, S.J. Micro-XRF Core Scanning in Palaeolimnology: Recent Developments. In *Micro-XRF Studies of Sediment Cores: Applications of a Non-Destructive Tool for the Environmental Sciences*; Croudace, I.W., Rothwell, R.G., Eds.; Springer: Dordrecht, The Netherlands, 2015; pp. 189–226.
55. Pakkad, G.; Elliott, S.; Anusarnsumthorn, V.; James, C.; Blakesley, D. Forest Restoration Planting in Northern Thailand. In *Proceedings of the Southeast Asian Moving Workshop on Conservation, Management and Utilization of Forest Genetic Resources No. 31/2002*; Food and Agriculture Organization of the United Nations: Bangkok, Thailand, 2002.
56. Natascha, W.; Setyaningsih, C.A.; Saad, A.; Sabiham, S.; Sauer, D.; Behling, H. Late Holocene volcanic and human impacts on the mountain vegetation in central Sumatra, Indonesia. *Quat. Int.* **2022**, *622*, 77–88. [CrossRef]
57. Erin, L.T.; André Luiz, G.; Sergio, R.-N.; Santiago, M.; George, D.W. Phylogeny of the Cecropieae (Urticaceae) and the Evolution of an Ant-Plant Mutualism. *Syst. Bot.* **2016**, *41*, 56–66. [CrossRef]
58. Michon, G.; Foresta, H.D. Agro-Forests: Incorporaing a Forest Vision in Agroforestry. In *Agroforestry in Sustainable Agricultural Systems*; Buck, L.E., Lassoie, J.P., Fernandes, E.C.M., Eds.; CRC Press: Boca Raton, FL, USA, 1999.
59. Berkes, F.; Folke, C.; Gadgil, M. Traditional Ecological Knowledge, Biodiversity, Resilience and Sustainability. In *Biodiversity Conservation: Problems and Policies*; Perrings, C.A., Mäler, K.G., Folke, C., Holling, C.S., Jansson, B.O., Eds.; Springer: Dordrecht, The Netherlands, 1995; pp. 281–299.
60. Michon, G.; Mary, F.; Bompard, J. Multistoried agroforestry garden system in West Sumatra, Indonesia. *Agrofor. Syst.* **1986**, *4*, 315–338. [CrossRef]
61. Flenley, J.R. Palynological Evidence for Land Use Changes in South-East Asia. *Journal of Biogeography* **1988**, *15*, 185–197. [CrossRef]
62. Elberson, W.; Oyen, L. *Sugar Palm (Arenga Pinnata)*; Wageningen University: Wageningen, The Netherlands, 2010.
63. Conedera, M.; Tinner, W.; Neff, C.; Meurer, M.; Dickens, A.F.; Krebs, P. Reconstructing past fire regimes: Methods, applications, and relevance to fire management and conservation. *Quat. Sci. Rev.* **2009**, *28*, 555–576. [CrossRef]
64. Torquebiau, E. Man-made dipterocarp forest in Sumatra. *Agrofor. Syst.* **1984**, *2*, 103–127. [CrossRef]
65. Meinwald, J.; Messer, A. *Anti-Insectan Compounds from the Tropical Tree Family Dipterocarpaceae*; United States Agency for International Development, Program in Science and Technology Cooperation, Cornell University: Ithaca, NY, USA, 1990.
66. Foresta, H.D.; Michon, G.; Kusworo, A.; Levang, P. Damar agroforests in Sumatra, Indonesia: Domestication of a forest ecosystem through domestication of dipterocarps for resin production. In *Forest Products, Livelioods and Coversation*; Kusters, K., Belcher, B., Eds.; Center for International Forestry Research: Jakarta, Indonesia, 2004; Volume 1—Asia.
67. Michon, G.; Foresta, H.D.; Levang, P. New face for traditional commons: Forest conversion and the redefinition of common property and individual rights through agroforest development in Sumatra, Indonesia. In Proceedings of the Fifth Common Property Conference, Bodø, Norway, 24–28 May 1995.
68. Watson, C.W. Kerinci, Two Historical Studies. Center of S.E.A Studies, University of Kent: Canterbury, UK, 1984; Volume 3.
69. van der Kaars, S.; Bassinot, F.; De Deckker, P.; Guichard, F. Changes in monsoon and ocean circulation and the vegetation cover of southwest Sumatra through the last 83,000years: The record from marine core BAR94-42. *Palaeogeogr. Palaeoclimatol. Palaeoecol.* **2010**, *296*, 52–78. [CrossRef]

70. Poffenberger, M. *Communities and Forest Management in Southeast Asia*; International Union for Conservation of Nature (IUCN): Gland, Switzerland, 1999.

71. Marsden, W. *The History of Sumatra: Containing an Account of the Government, Laws, Customs, and Manners of the Native Inhabitants*; Cambridge University Press: Cambridge, UK, 2012.

72. Foresta, H.D.; Michon, G. Damar resin: Indonesia case. In *Riches of the Forest: Food, Spices, Crafts and Resins of Asia*; López, C., Shanley, P., Eds.; Center for International Forestry Research: Bogor Regency, Indonesia, 2004.

73. Pino, J.; Arnan, X.; Rodrigo, A.; Retana, J. Post-fire invasion and subsequent extinction of *Conyza* spp. in Mediterranean forests is mostly explained by local factors. *Weed Res.* **2013**, *53*, 470–478. [CrossRef]

74. Kołaczek, P.; Zubek, S.; Błaszkowski, J.; Mleczko, P.; Margielewski, W. Erosion or plant succession—How to interpret the presence of arbuscular mycorrhizal fungi (Glomeromycota) spores in pollen profiles collected from mires. *Rev. Palaeobot. Palynol.* **2013**, *189*, 29–37. [CrossRef]

75. Biagioni, S.; Krashevska, V.; Achnopha, Y.; Saad, A.; Sabiham, S.; Behling, H. 8000 years of vegetation dynamics and environmental changes of a unique inland peat ecosystem of the Jambi Province in Central Sumatra, Indonesia. *Palaeogeogr. Palaeoclimatol. Palaeoecol.* **2015**, *440*, 813–829. [CrossRef]

76. Chen, S.; Hoffmann, S.S.; Lund, D.C.; Cobb, K.M.; Emile-Geay, J.; Adkins, J.F. A high-resolution speleothem record of western equatorial Pacific rainfall: Implications for Holocene ENSO evolution. *Earth Planet. Sci. Lett.* **2016**, *442*, 61–71. [CrossRef]

77. Koutavas, A.; Joanides, S. El Niño–Southern Oscillation extrema in the Holocene and Last Glacial Maximum. *Paleoceanography* **2012**, *27*, 1–15. [CrossRef]

78. Zeist, W.v.; Polhaupessy, N.A.; Stuijts, I.M. Two pollen diagrams from west Java, a preliminary report. *Mod. Quat. Res. S.E. Asia* **1979**, *5*, 43–56.

79. Shen, X.; Liu, B.; Henderson, M.; Wang, L.; Jiang, M.; Lu, X. Vegetation Greening, Extended Growing Seasons, and Temperature Feedbacks in Warming Temperate Grasslands of China. *J. Clim.* **2022**, *35*, 5103–5117. [CrossRef]

80. Shen, X.; Liu, Y.; Liu, B.; Zhang, J.; Wang, L.; Lu, X.; Jiang, M. Effect of shrub encroachment on land surface temperature in semi-arid areas of temperate regions of the Northern Hemisphere. *Agric. For. Meteorol.* **2022**, *320*, 108943. [CrossRef]